Coulomb Stress Analysis of the 21 February 2008 M_w= 6.0 Wells, Nevada, Earthquake

by

Volkan Sevilgen
U. S. Geological Survey, Menlo Park, CA

2011

ABSTRACT

Static Coulomb stress changes imparted by the February 21, 2008 Wells, Nevada earthquake are calculated, using an 8 x 6 km rectangular patch with a uniform slip as a source fault. Stress changes are resolved on nearby active faults using their rake, dip, and strike direction, assuming a fault friction of 0.4. The largest Coulomb stress increase (0.2 bars) imparted to surrounding major active faults from the Wells earthquake occurs on the Clover Hill fault, which may be the southern continuation of the ruptured fault. A 0.1 bar Coulomb stress increase is calculated on the western Snake Mountains fault. Coulomb stress decreases of 0.5 bars are calculated for the northern parts of the Independence and Ruby Mountains faults. The Coulomb stress change is calculated on relocated aftershocks assuming that they have the same strike, dip, and rake, as the source fault. Under this assumption, 75% of the aftershocks received a Coulomb stress increase.

INTRODUCTION

The M_w= 6.0 Wells, Nevada, earthquake struck beneath Town Creek Flat, near the southern end of the Snake Mountains and north of the Wood Hills (figure 1A). The active faults in the study area, which are located in the Basin and Range Province, are assumed to have a dip of about 60° and to have normal dip-slip movement. The Clover Hill fault and the earthquake source fault dip to the east, and the rest of the faults modeled dip to the west. The central and northern Ruby Mountains faults have ruptured within the last 15,000 years and have a slip rate of 0.2-0.5 mm/year [U.S. Geological Survey (USGS), 2006]. The Independence fault has ruptured within the last 130,000 years and has a slip rate of 0.2-0.5 mm/year (USGS, 2006).

METHODOLOGY

The computer program Coulomb 3.1 (Lin and Stein, 2004; Toda and others, 2005; Toda and others, 2007) is used to calculate the static Coulomb stress change (figure 1B), shear stress change (figure 2A), and fault-normal stress change (figure 2B) on active fault planes to understand the changes of earthquake potential on the surrounding faults. A fault friction coefficient of 0.4 is assumed in an elastic half-space model (c.f., King and others, 1994).

I used aftershocks relocated by Ken Smith of the Nevada Seismological Laboratory (2008, written communication), to infer the location and geometry of the source fault with a strike of 35° and a 55°E dip (figures 3A and 3B). Based on the observed hole in the seismicity, an 8 x 6 km rectangular source fault is assumed between 4.5 and 9.5 km depths (figure 3B). Using -83° rake from the USGS focal mechanism, 0.76 m normal and 0.09 m left-lateral slip is calculated to produce an earthquake with a seismic moment of M_o= 1.18 e+25 dyne cm, and an earthquake magnitude of M_w= 6.0.

Figure 1A. Topography with active fault traces from Quaternary fault database (USGS, 2006).
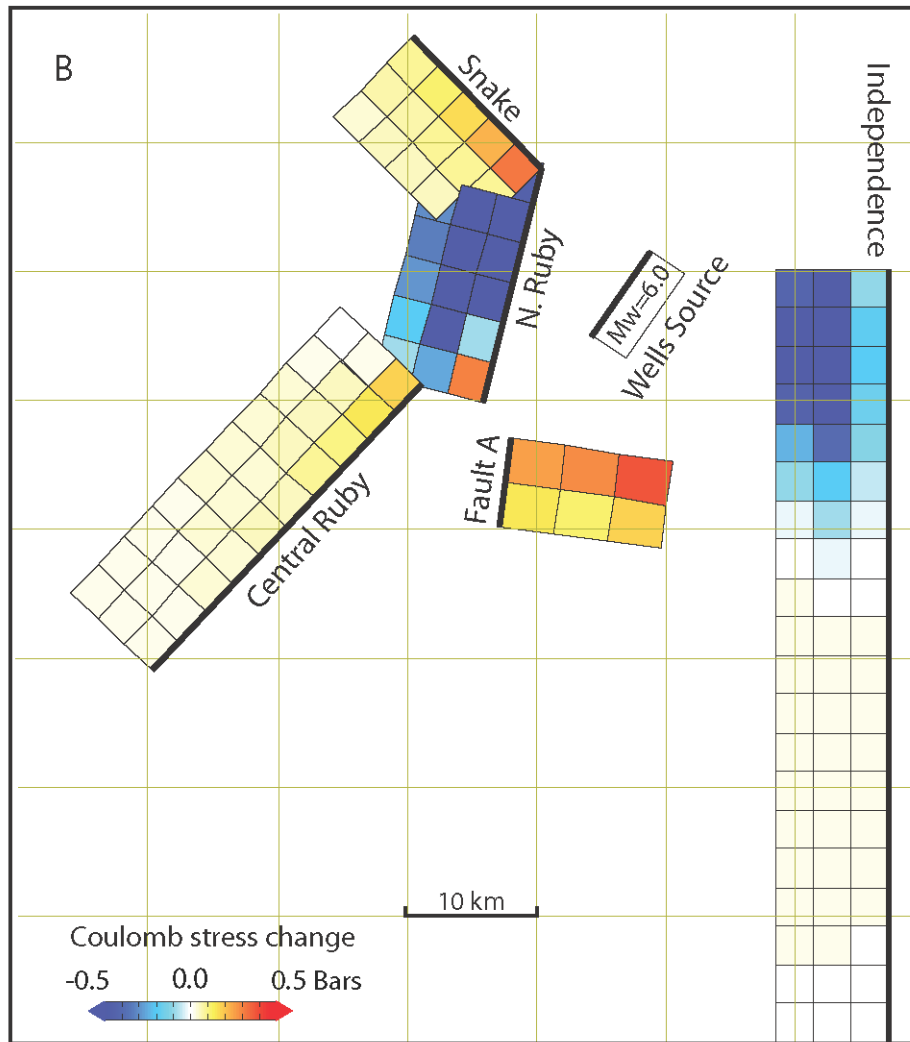
Figure 1B. Coulomb stress changes on modeled faults from the Wells earthquake. The source fault (rectangle) has a 35° strike, 55° NW dip, and -83° rake. Receiver faults: Fault A is the Clover Hill fault modeled as a 55°-east-dipping normal fault, and other faults are modeled as 60°-west-dipping normal faults. Fault friction assumed 0.4. The red colors are increased Coulomb stresses, the blue colors are decreased Coulomb stresses, and the white areas are sections of the faults are where there are no stress changes.
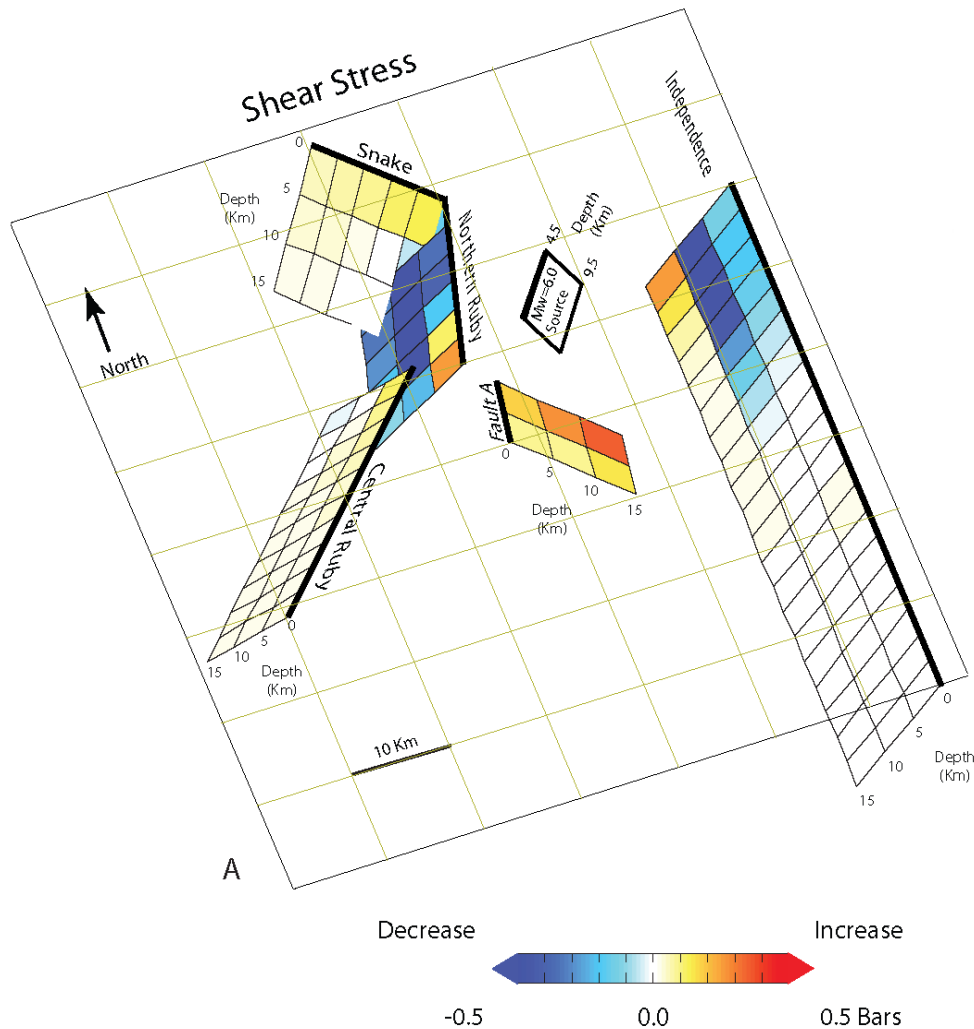
Figure 2A. Shear stress changes on modeled faults.

COULOMB STRESS CHANGES ON ACTIVE FAULT PLANES

The changes in Coulomb stress on nearby faults that were created by the Wells earthquake are shown in figures 1 and 2. Such stress changes have been demonstrated to be useful in explaining the occurrence of local seismicity following major earthquakes (e.g., Stein, 1999). The Clover Hill fault, which strikes 8° and dips 50° to the east, has the largest Coulomb stress increase, with an average of 0.22 bars (figure 1B), because of decreases in fault-normal stresses and a shear stress increase. This small fault is important because it might be the southern extension of the 2008 earthquake rupture plane. The southern portion of the western Snake Mountains fault, which was modeled with a strike of 135° and a 60° westward dip, has a Coulomb stress increase with an average 0.1 bars. The shallow portion of the northernmost central Ruby Mountains fault (modeled as a fault with a strike of 225° and a westward dip of 60˚) has a negligible Coulomb stress increase (< 0.05 bars) (figure 1B).

A large Coulomb stress decrease of 0.5 bars is calculated on the northern portion of the Independence fault, which is modeled as a normal fault with a strike of 180° and a westward dip of 60° (figure 1B), largely because of increased fault-normal stress across the deeper parts of the fault (figure 2B) and shear stress decrease on shallow parts. The southern portion has a negligible Coulomb stress increase (< 0.05 bars). The northern Ruby Mountains fault also has a large Coulomb stress decrease by 0.5 bars, which is likely to inhibit Coulomb failure on the 195°-striking and 60°-west-dipping normal fault, both because of an increase of normal stress across the fault (0.57 bars) and a shear stress decrease (0.35 bars).
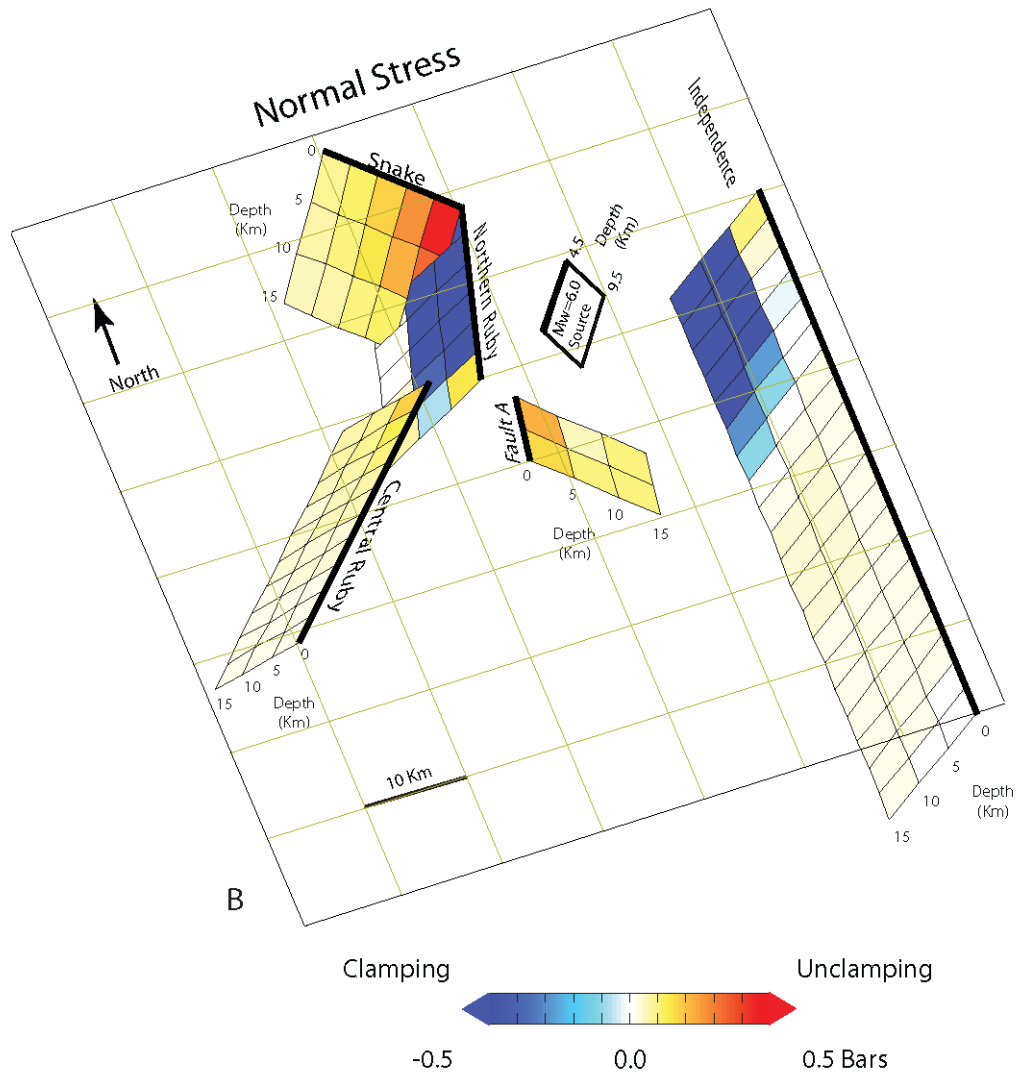
Figure 2B. Fault-normal stress changes on modeled faults. Fault A is the Clover Hill fault. The red colors are increased stresses, the blue colors are decreased stresses, and the white areas are sections of the faults are where there are no stress changes.

COULOMB STRESS CHANGES ON AFTERSHOCKS

Coulomb stress changes from the Wells earthquake model were calculated for aftershocks to investigate whether they were the result of increased stresses from the mainshock (c.f., Stein and Lisowski, 1983). Assuming that this source model and the aftershocks have the same strike, dip, and rake as the mainshock, 75% of the 870 aftershocks as of August 12, 2008 were brought closer to failure by the main rupture (figure 3A and 3B). A cluster of aftershocks on the corner of the assumed source plane (figure 3A and 3B), received a Coulomb stress change decrease, perhaps because the assumed fault planes and uniform slip model are too simple.
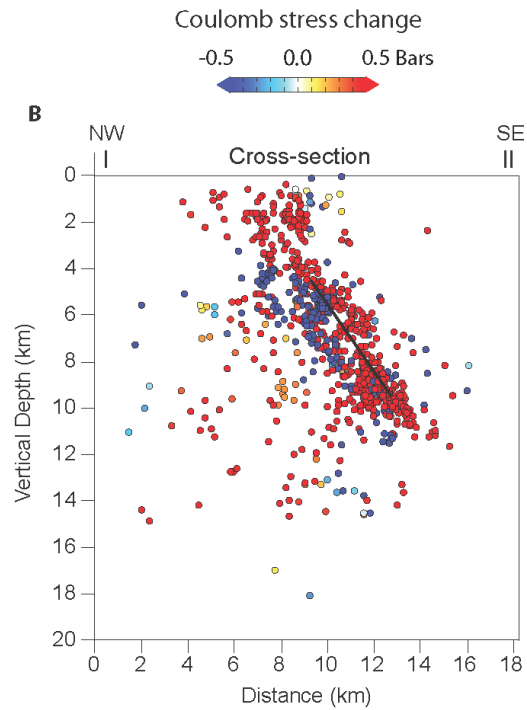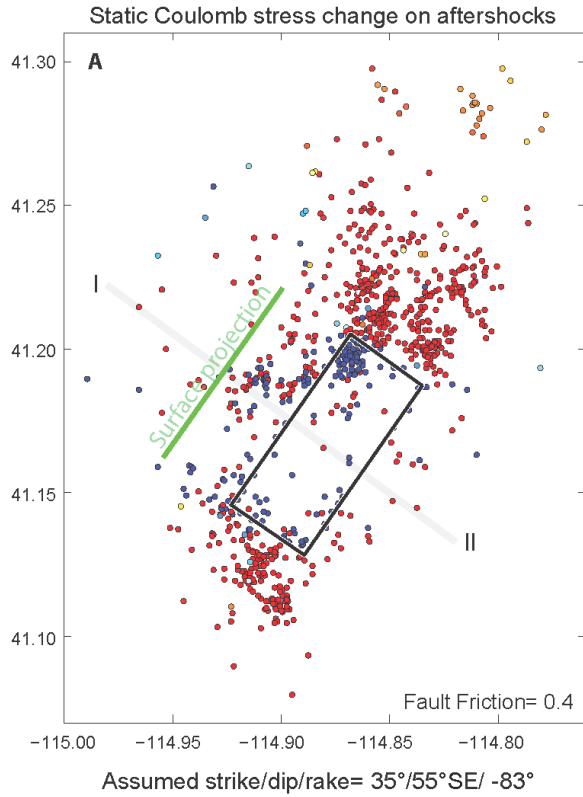
Figure 3A. Coulomb stress changes on aftershocks, assumed to have the same strike, dip rake as mainshock. Friction coefficient is 0.4. The red-colored aftershocks have an increased Coulomb stress change and the blue-colored aftershocks have a coulomb stress decrease.

Figure 3B. Cross section of aftershocks viewed along the assumed Wells earthquake plane.

CONCLUSIONS

The greatest Coulomb stress effect imparted from Wells earthquake was an increase in shear stress and a decrease in fault-normal stress across the Clover Hill fault, moving that fault closer towards failure. A modest promotion towards failure is seen along the southern part of the western Snake Mountains fault, whereas there was a negligible increase for the shallow depths of the northernmost part of the central Ruby Mountains fault. The Coulomb stress decrease is indicated on the northern part of the Independence fault and the northern Ruby Mountains fault that inhibits Coulomb failure.

Using simple assumptions, 75% of the aftershocks of the Wells earthquake over the first six months had increases of Coulomb stress from the 2008 earthquake, indicating they were likely related to, or triggered by, the mainshock.

Further monitoring and microseismicity studies should reveal whether the calculated stress increases are associated with seismicity rate increases, which, if found, might indicate an increased earthquake hazard.

ACKNOWLEDGMENTS

I thank Ross Stein and Jeanne Hardeback for reviews.

REFERENCES

King, G.C.P., Stein, R.S., and Lin, J., 1994, Static stress changes and the triggering of earthquakes: Bulletin of the Seismological Society of America, v. 84, p. 935–953.

Lin, J. and Stein, R.S., 2004, Stress triggering in thrust and subduction earthquakes, and stress interaction between the southern San Andreas and nearby thrust and strike-slip faults: Journal of Geophysical Research, v. 109, B02303, doi:10.1029/2003JB002607.

Stein, R.S., 1999, The role of stress transfer in earthquake occurrence: Nature, v. 402, p. 605–609.

Stein, R.S. and Lisowski, M., 1983, The 1979 Homestead Valley earthquake sequence, California–Control of aftershock and postseismic deformation: Journal of Geophysical Research, v. 88, p. 6477–6490.

Toda, S., Stein, R.S., Richards-Dinger, K., and Bozkurt, S., 2005, Forecasting the evolution of seismicity in southern California– Animations built on earthquake stress transfer: Journal of Geophysical Research, v.110, B05S16, doi:10.1029/2004JB003415.

Toda, S., Stein, R.S., Lin, J., Sevilgen, V., 2007, Coulomb 3.1 Software: USGS Stress Triggering Group.

U.S. Geological Survey, 2006, Quaternary fault and fold database for the United States, accessed Jan 9, 2006, from USGS web site: http//earthquake.usgs.gov/regional/qfaults/